RSC Advances

PAPER

View Article Online
View Journal | View Issue

Cite this: *RSC Adv.*, 2023, **13**, 21421

Is acriflavine an efficient co-drug in chemotherapy?

Kinga Piorecka, *[a] Jan Kurjata, [a] Bartłomiej Gostynski, [a] Slawomir Kazmierski, [a] Wlodzimierz A. Stanczyk, [a] Monika Marcinkowska, [b] Anna Janaszewska [b] and Barbara Klajnert-Maculewicz [b]

Cancer is a global health problem being the second worldwide cause of deaths right after cardiovascular diseases. The main methods of cancer treatment involve surgery, radiation and chemotherapy with an emphasis on the latter. Thus development of nanochemistry and nanomedicine in a search for more effective and safer cancer treatment is an important area of current research. Below, we present interaction of doxorubicin and acriflavine and the cytotoxicity of these drug nano-complexes towards cervical cancer (HeLa) cells. Experimental results obtained from NMR measurements and fluorescence spectroscopy show that the drugs' interaction was due to van der Waals forces, formation of hydrogen bonds and $\pi-\pi$ stacking. Quantum molecular simulations confirmed the experimental results with regard to existing $\pi-\pi$ stacking. Additionally it was shown that, at the level of theory applied (DFT, triple zeta basis set), the stacking interactions comprise the most preferable interactions (the lowest ΔG *ca.* -12 kcal mol^{-1}) both between the molecules forming the acriflavine system and between the other component – another drug (doxorubicin) dimer. Biological tests performed on HeLa cells showed high cytotoxicity of the complexes, comparable to free drugs (ACF and DOX), both after 24 and 48 hours of incubation. For non-cancerous cells, a statistically significant difference in the cytotoxicity of drugs and complexes was observed in the case of a short incubation period. The results of the uptake study showed significantly more efficient cellular uptake of acriflavine than doxorubicin, whether administered alone or in combination with an anthracycline. The mechanism determining the selective uptake of acriflavine and ACF : DOX complexes towards non-cancer and cancer cells should be better understood in the future, as it may be of key importance in the design of complexes with toxic anti-cancer drugs.

Received 19th April 2023
Accepted 6th July 2023

DOI: 10.1039/d3ra02608f

rsc.li/rsc-advances

Introduction

Despite the progress of medicine and science in improving anticancer therapy, cancer is still one of the most deadly diseases in the world. Appropriate targeted drug delivery systems are being sought for higher efficiency and selectivity. The main goal could be targeting drugs to the cancer cell DNA. This is the so-called DNA intercalation process in which the drug, by changing the conformation of the double-stranded DNA, is "inserted" between sequential base pairs, leading to a change in the sugar-phosphate backbone.[1]

Doxorubicin (DOX) is an intercalating drug widely used in anti-cancer therapy to treat acute leukemia, malignant lymphoma, breast cancer, ovarian cancer, and cervical cancer among others.[2,3] DOX inhibits topoisomerase II leading to double-stranded DNA breaks or DNA intercalation resulting in apoptosis of cancer cells.[4,5] Unfortunately, long-term administration of doxorubicin is associated with side effects related to high toxicity to healthy tissues. In particular, cardiotoxicity and tumor resistance are recognized as the main problems of this therapy.[6,7] Cancer cells can initiate appropriate defense mechanisms to prevent the anti-cancer immune response and can survive under conditions of hypoxia.[8] This is due to, *inter alia*, overexpression of the hypoxia-induced factor (HIF-1α), which regulates the expression of factors involved in tumor metabolism (GLUT1), angiogenesis (VEGF), metastasis and promoting Epithelial-to-Mesenchymal Transition (EMT).[9–11] The use of high doses of doxorubicin may cause also oxidative stress,[12] resulting in increased levels of reactive oxygen species (ROS), and consequently overexpression of HIF-1α in tumor cells, promoting drug resistance and tumor progression.[13] To prevent this, it can be appropriate to use an effective HIF-1 inhibitor in the therapy of doxorubicin.

Acriflavine (ACF) has been recognized as the most potent HIF-1 inhibitor in anti-cancer therapy among the 336 drugs approved by the Food and Drug Administration.[14] ACF has been known in the literature since 1912 as an antibacterial drug and currently is recognized as a potential anti-SARS-CoV2 and anti-cancer drug.[15,16] Acriflavine is a mixture of trypaflavine and proflavine,[17] having a flat aromatic system[18] that makes it, like doxorubicin, a DNA intercalator.[19–25] The multitasking nature of

[a]*Centre of Molecular and Macromolecular Studies, Polish Academy of Sciences, Sienkiewicza 112, Lodz, 90-363, Poland. E-mail: kinga.piorecka@cbmm.lodz.pl*
[b]*Department of General Biophysics, Faculty of Biology and Environmental Protection, University of Lodz, 141/143 Pomorska St., 90-236 Lodz, Poland*

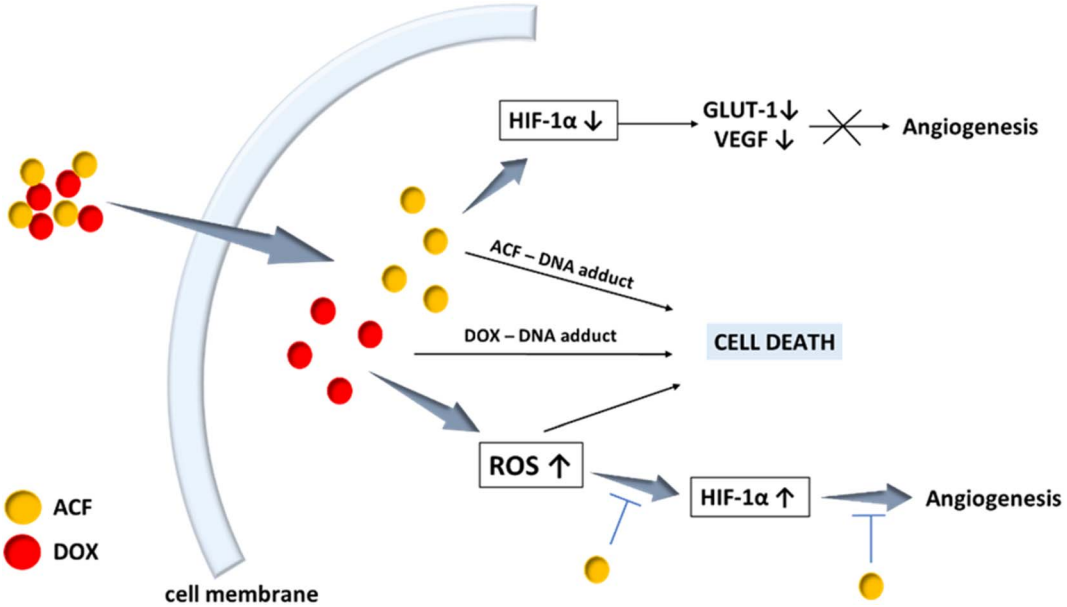

Fig. 1 The proposed mechanism of action of the ACF : DOX complex in the fight against cancer.

acriflavine has been recently reviewed.[26] ACF has been reported to be an effective drug against a wide spectrum of cancers, including breast cancer,[27] colon cancer,[28] pancreas,[29] cervix,[30] brain cancer[31] and melanoma.[32] The use of acriflavine may be important, first of all, in the treatment of solid tumors, such as cervical cancer, for which the level of hypoxia (determining the malignancy of the tumor) is high. Acriflavine blocks HIF-1, which is responsible for hypoxia, and therefore it can sensitize the tumor to radiotherapy,[33] chemotherapy[34] and photodynamic therapy (Fig. 1).[30]

Acriflavine is highly ionized and soluble in water.[21] There are reports that acriflavine may interact with other drugs or substances. Depending on the conditions (pH, type of solvent, *etc.*), acriflavine may interact through hydrogen bonding, van der Waals, ionic and hydrophobic bonds. For example acriflavine is known to form ion pair complexes *via* electrostatic interactions with such the drugs as ketoprofen, diclofenac sodium,[35] tranilast,[36] olsalazine and sulfasalazine.[37] Moreover, acriflavine can form an ion association complex with tartrazine in an acidic environment at pH 3.75, due to the presence of a carboxyl group in the structure of these drugs, where acriflavine can dissociate as a positively charged cation ($-N^+$), and tartrazine can exist as two negatively charged anions ($-SO^{3-}$). Other studies indicate the presence of hydrogen interactions and van der Waals forces between acriflavine and uracils.[38] It can also form complexes with drugs that contain hydroxyl groups. Examples are: the ionic complex of ascorbic acid and acriflavine at pH 6 (ref. 39) and the ACF inclusion complex with α-CD favored by the van der Waals force at pH 7.4.[40] The presence of nitrogen atoms in ACF allows the potential molecule to interact with estrogens having hydroxyl groups through hydrogen bonding.[41]

Most of the scientific works on the interaction of acriflavine with other substances concerned the recognition of acriflavine as a fluorimetric reagent for the determination of these compounds. Thus, fluorimetric testing can be a quick way for obtaining information concerning the interaction of acriflavine with drug carriers or other systems, which can be used to design new drug systems.

The concept of placing DOX and ACF in a liposomal carrier is known in the literature, which gives better results than single drugs in the treatment of colorectal cancer.[42] However, no one has previously studied the direct interaction of DOX with ACF and its effect on cancer cells. Such knowledge could be a tool for the development of future combined therapy and for better understanding of the role of acriflavine in order to design better nano-systems systems in biomedicine.

On the other hand, combination chemotherapy is currently most often practiced in the treatment of cancer. Despite the continuous development towards the creation of new drug delivery systems, there are still barriers to their application. This is due to additional FDA approvals, the use of auxiliary material and a complicated manufacturing procedure. Therefore, great emphasis is placed on the development of "green" strategies for the production of drug systems.[43]

In this work, we describe the acriflavine–doxorubicin complex as a multitasking platform in the fight against cancer. The advantage of this concept is the use of drugs in an unchanged form that is approved for use in medicine. The use of spectrofluorimetry and NMR studies allowed us to evaluate the interactions between doxorubicin and acriflavine. The most important goal of these studies was to assess the biological activity of these complexes against cervical cancer cells.

Results and discussion

Fluorescence and NMR analysis

In spectrofluorimetric studies, the formation of complexes between acriflavine and doxorubicin (quencher) can be

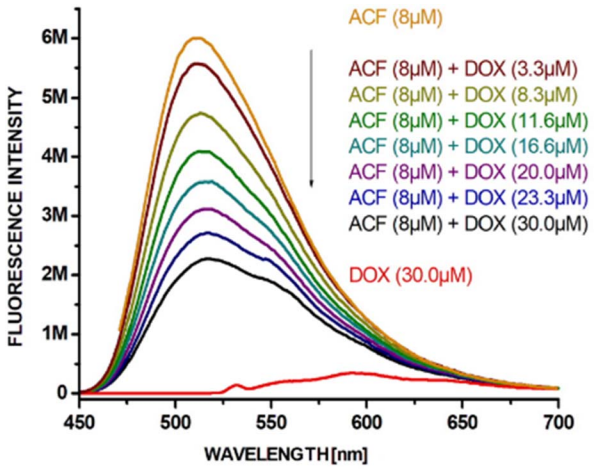

Fig. 2 Effect of doxorubicin concentration (0–30 μM) on the fluorescence intensity of acriflavine (8 μM). The arrow indicates that the emission intensity is decreasing as the DOX concentration increases.

observed by changing the intensity of fluorescence. Acriflavine fluoresces at 512 nm after excitation at 265 nm. The fluorescence intensity of acriflavine decreased after complex formation with doxorubicin. Fig. 2 shows the quenching of AFN fluorescence in the presence and absence of DOX at various concentrations. The higher the concentration of added doxorubicin (0–30 μM) to the aqueous ACF solution (at a constant concentration of ACF, 8 μM), the lower the intensity of fluorescence. Based on the literature,[38,41] it can be assumed that the van der Waals forces and the hydrogen bonds formed between the aromatic hydroxyl groups of doxorubicin and the amino groups of acriflavine are related to the quenching phenomenon.

Based on our previous publications, the interaction of doxorubicin with the carriers can be studied by NMR spectroscopy.[44–47] NMR can determine which protons are involved in the interaction of ACF with DOX and help determine the type of interaction. To determine the involvement of protons of the hydroxyl groups, the ^{1}H NMR spectra of the pure doxorubicin solution and the doxorubicin–acriflavine mixture solution (Fig. 3C) in an aprotic solvent (DMSO-d6) were superimposed. A disappearance or broadening of the signals from the protons of the hydroxyl groups at the aromatic (Ar-OH) moieties of doxorubicin as a result of their interaction with acriflavine was observed. In other words, the Ar-OH groups of doxorubicin are involved in the formation of a complex with acriflavine. To establish other interactions, the ROESY experiment was performed in the same solvent. The ROESY experiment allows one to observe the correlation between molecules of any mass and determines which signals come from protons that are close to each other. ROESY NMR measurements for the mixture of acriflavine and doxorubicin allowed us to determine which ACF and DOX protons interact with each other on the basis of cross peaks. It has been established that there is π–π stacking between these drugs on the basis of cross peaks derived from the aromatic protons of doxorubicin (1–3) and acriflavine (a, h) (Fig. 3G). Additionally, cross peaks from other aromatic protons of doxorubicin (1, 2) and acriflavine (b, g) were observed, which confirms the presence of π–π stacking.

The studies conducted so far in DMSO-d6 do not, unfortunately, provide a complete answer to whether the same interactions will be obtained in aqueous solutions used in the administration of drugs *via* the intravenous route. Therefore, the experiment was also carried out in deuterated water (0.9% saline). Due to the protic nature of water, unfortunately we were unable to obtain results for the interaction of protons of the hydroxyl groups. Only the π–π interactions were visible, observation on the basis of cross-peaks originating from doxorubicin protons (1, 3) with acriflavine protons (a, h) in the ROESY spectrum (Fig. 3E) and changes in chemical shifts of signals originating from aromatic protons of both drugs and the –OCH_3 group in the ^{1}H NMR spectrum (Fig. 3F).

The ACF : DOX complex was also characterized by Diffusion-Ordered Spectroscopy (DOSY) NMR (Fig. 3D). DOSY is a technique that evaluates the diffusion coefficient for individual resonances in NMR spectra. Most often, DOSY is used to measure the average size of a polymer,[48] but in this study we wanted to see if both drugs would have the same diffusion coefficient, which could indicate an interaction of acriflavine with doxorubicin. To confirm this, we prepared aqueous solutions (0.9% saline) of a mixture of acriflavine and doxorubicin and pure ACF with the same concentrations. Fig. 3D shows the superimposed spectra of the complex and of pure acriflavine to visualize the change in the diffusion coefficient. The complex signals of both drugs show equivalent diffusion coefficients of $\sim 1.45 \times 10^{-10}$ m^2 s^{-1}, while acriflavine alone has a diffusion coefficient of $\sim 2.39 \times 10^{-10}$ m^2 s^{-1} w D_2O (0.9% saline). Based on the Stokes–Einstein equation, the hydrodynamic radius of the ACF : DOX complex was estimated to be ~1.7 nm, while for free acriflavine it was less than ~1 nm.

Summing up, the NMR results confirm that acriflavine–doxorubicin complex was formed in water through the involvement of π–π interactions and hydrogen bonds.

Computational studies

The main goal of the computational research was to investigate the DOX–ACF system's ability to form hydrogen bond and π–π stacking interactions. Due to the large system size, the energy optimizations were initially performed by means of semi-empirical PM6 method and subsequently refined by DFT calculations with hybrid B3LYP functional with GD3 empirical correction term (B3LYP-GD3/6-311 + G(d)//B3LYP-GD3/6-31 + G(d) calculations).[49,50] Size of the system was the main reason for the modest basis set size. The SCRF solvent (water) was modelled using the continuum solvation model (CPCM) as implemented in the Gaussian 16 set of codes.[51] The basis set superposition error was also calculated for the gas phase as G16 does not support such calculations for SCRF computations.[52]

The size of the system and the associated calculation time was also the reason for some abridgement of the systems in question and the cases of interaction between them due to the fact that acriflavine appears on sale as a mixture of an active compound (a chloride salt, henceforth referred to as: Me-ACF)

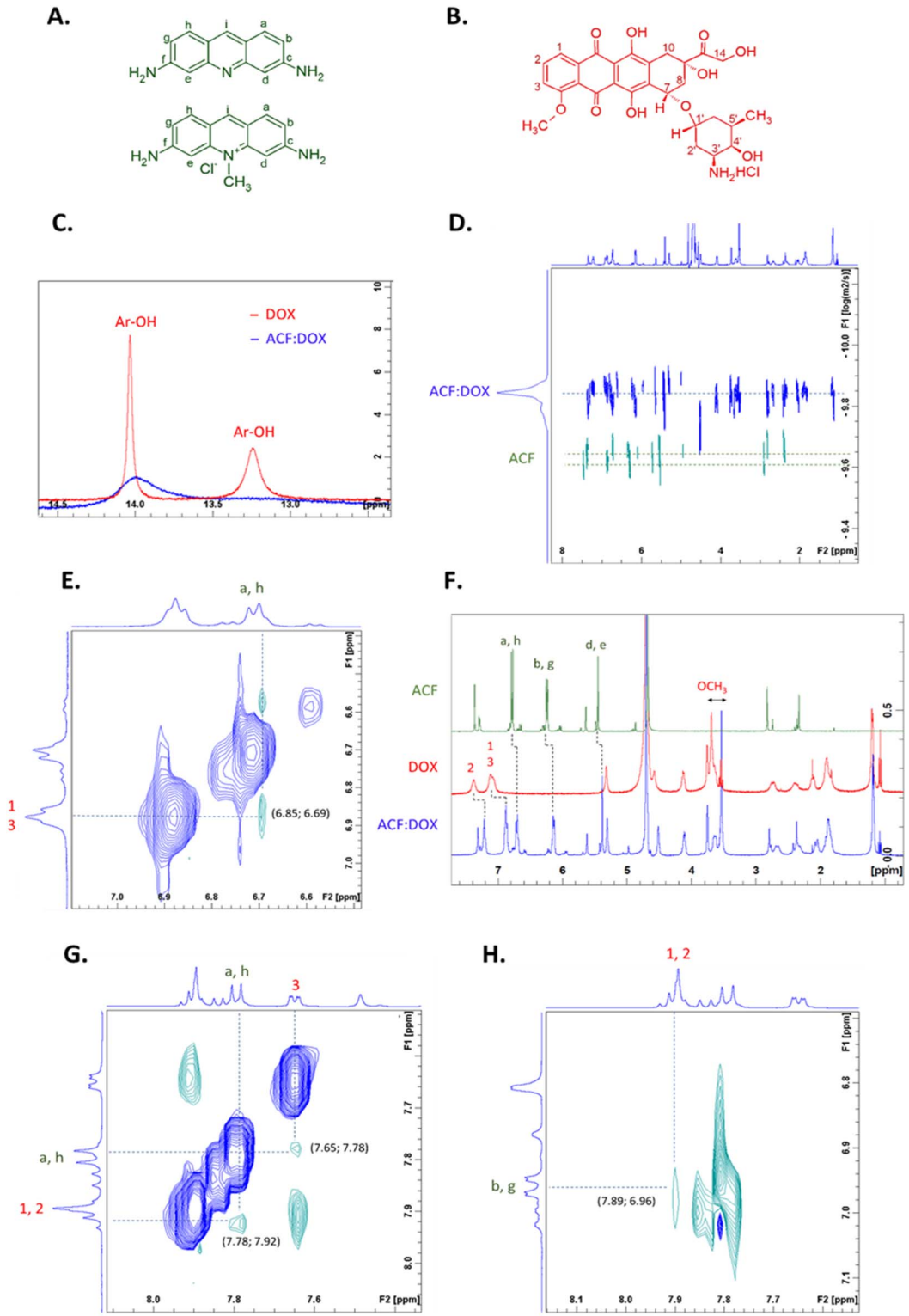

Fig. 3 A Structure of acriflavine (ACF). (B) Structure of doxorubicin (DOX). (C) Superimposition of the ^{1}H NMR (DMSO-d6, 400 MHz) spectrum of the substrate – doxorubicin on the spectrum of the product – ACF : DOX complex. The disappearance and broadening of the signal from the Ar-OH protons is due to the formation of hydrogen bonds between DOX and ACF. (D) Superimposition of the DOSY spectrum of the acriflavine on the spectrum of the ACF : DOX complex. The spectrum shows the change in the diffusion coefficient of acriflavine after complex formation with doxorubicin. (E) ROESY (D_2O, 400 MHz) spectrum of ACF : DOX complex: cross-correlation peaks for protons 1, 3 from doxorubicin and peaks for protons a, h from ACF were identified. (F) ^{1}H NMR spectra (D_2O, 400 MHz) of the ACF : DOX complex, doxorubicin and acriflavine: the dashed line indicates the change in chemical shifts derived from the protons of doxorubicin (1, 2, 3, OCH_3) and acriflavine (a, h, b, g, d, e) caused by the formation of the ACF : DOX complex. (G) ROESY (DMSO-d6, 400 MHz) spectrum of ACF : DOX complex: cross-correlation peaks for protons 1, 2, 3 from doxorubicin and peaks for protons a, h from ACF were identified. (H) ROESY (DMSO-d6, 400 MHz) spectrum of ACF : DOX complex: cross-correlation peaks for protons 1, 2 from doxorubicin and peaks for protons b, g from ACF were identified.

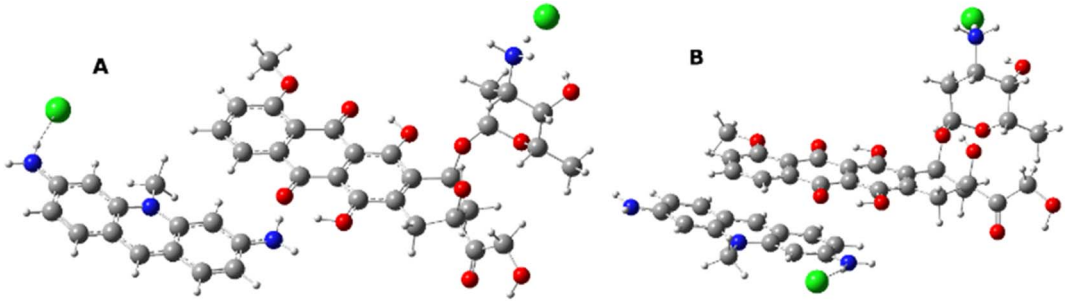

Fig. 4 Examples of initial geometries: (A) interactions of Me-ACF $-NH_2$ group with –OH of DOX; (B) $\pi-\pi$ interactions.

and a stabilizer (henceforth: ACF). Acriflavine interaction with doxorubicin (henceforth: DOX) and with itself were modeled as dimers as follows: ACF–ACF (homodimer of the stabilizer), Me-ACF–Me-ACF (homodimer of the active compound), ACF–Me-ACF (heterodimer stabilizer–active compound), ACF–DOX (heterodimer stabilizer–doxorubicin), Me-ACF–DOX (heterodimer active compound–doxorubicin). Trimolecular interactions (*e.g.* Me-ACF–DOX–ACF or ACF–Me-ACF–DOX or any other of their permutations) were considered statistically much less probable than dimer interactions. DOX–DOX interactions were omitted due to: the large size of the DOX molecule compared to Me-ACF and ACF molecules which size would significantly extend the calculation time for DOX homodimer and the experimental data suggesting that acriflavine aggregates with doxorubicin, and therefore formation of the acriflavine–doxorubicin dimer is certainly more preferred than the DOX–DOX interactions.

The results obtained suggest that the most energetically stable spatial arrangements of dimers are those stabilized by $\pi-\pi$ stacking (energy difference between various interaction modes are even about 14 kcal mol^{-1} in magnitude) and the systems' geometry in solution very often converges to such arrangements, independently from the starting position (Fig. 4 and 5) they were set to.

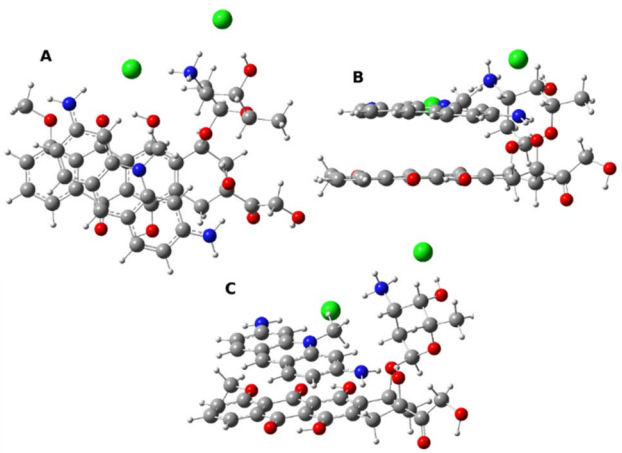

Fig. 5 The most energetically favored structure of the Me-ACF–DOX complex in the projection from above (A), from side (B) and oblique (C).

Calculation results of the Gibbs free energy of dimerization (Table 1) reveal that heterodimers are preferred over homodimers (the reference point was each time the sum of the Gibbs free energy of free isolated molecules forming the examined complex). Additionally, values of basis set superposition error (BSSE) calculated for the gas phase are presented.

Homodimerization of ACF is a process that is thermodynamically not favorable which is something to be expected from a molecule that is used primarily as a stabilizer for the active Me-ACF. Forming of the ACF–Me-ACF complex is slightly thermodynamically favorable but the Me-ACF dimer is the most energetically stable dimer among all possible combinations of acriflavine constituents. In support of the experimental results – calculations show that doxorubicin forms energetically favorable dimers (stabilized by $\pi-\pi$ interactions) with both acriflavine moieties and the active Me-ACF forms the most energetically favorable complexes of all the investigated ones.

Determination of cytotoxicity

The aim of the study was to compare the anticancer efficacy of free doxorubicin (DOX), acriflavine (ACF) and their three complexes in a molar ratio of 1 : 1, 1 : 2 and 1 : 5 on cancer (HeLa) and non-cancer (HMEC-1) cells. Compounds were added in the concentration range of 1, 5, 10, 50 μM, and the incubation time was 24 and 48 hours, respectively (Fig. 6, Table 2).

In the case of cancer cells, all complexes showed high cytotoxicity comparable to the free drugs (ACF and DOX), especially at higher concentrations after 24 and in all concentration ranges after 48 hours of incubation. Comparing the bars representing the viability of HeLa cancer cells and non-cancerous HMEC-1 cells, all complexes were less toxic to non-cancerous

Table 1 Values of the Gibbs free energy of dimerization for the investigated compounds and their corresponding gas-phase BSSE

Complex	ΔG_{compl} [kcal mol^{-1}]	BSSE [kcal mol^{-1}]
ACF–ACF	1.6	2.8
ACF –Me-ACF	−0.2	4.0
Me-ACF–Me-ACF	−5.2	4.0
ACF–DOX	−4.9	4.7
Me-ACF–DOX	−12.2	6.4

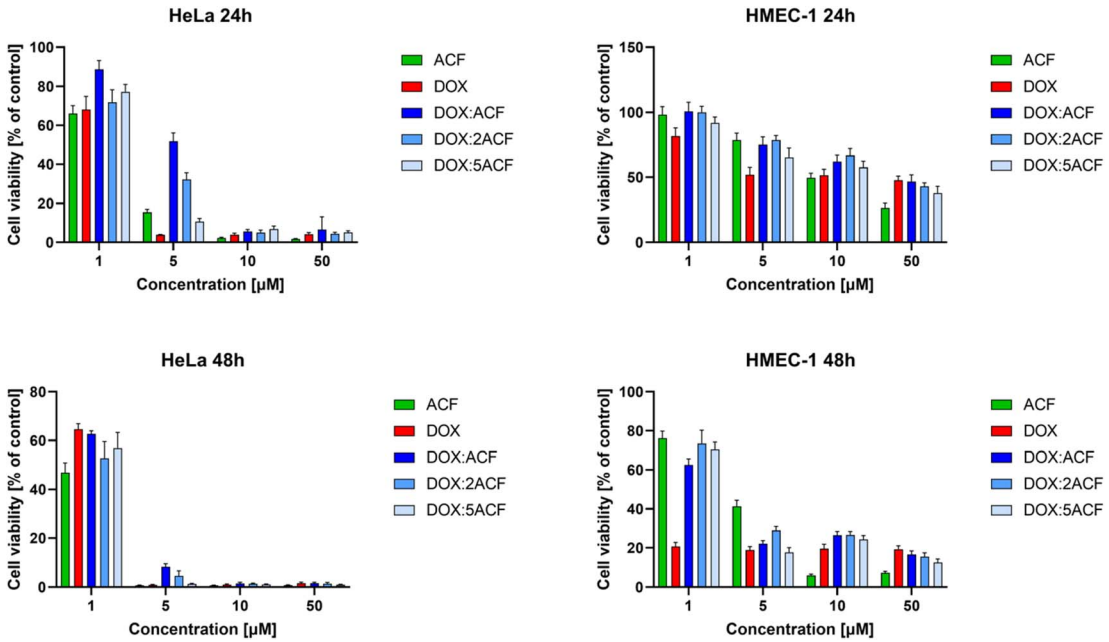

Fig. 6 The influence of the doxorubicin (DOX), acriflavine (ACF) and their complexes in molar ratios 1 : 1, 1 : 2 and 1 : 5 on viability of human cervical cancer endothelial (HeLa) cells after and dermal microvascular endothelium (HMEC-1) cells after 24 h (upper panel) and 48 h (lower panel) incubation in a 310 K. Data are presented as a percentage of control (untreated cells) ± standard deviation (SD).

Table 2 Comparison of IC_{50} value for doxorubicin (DOX), acriflavine (ACF) and their complexes in molar ratios 1 : 1, 1 : 2 and 1 : 5 in HeLa and HMEC-1 cell lines. The IC_{50} values are presented as mean ± SD. The statistical significance was assessed between free DOX and three complexes (*$p < 0.05$, **$p < 0.01$, ***$p < 0.005$) as well as free ACF and three complexes at the IC_{50} concentration point ($^{\#}p < 0.05$, $^{\#\#}p < 0.01$, $^{\#\#\#}p < 0.005$)

	HeLa		HMEC-1		
IC_{50} [μM]	24 h	48 h	24 h		48 h
DOX	1.068 ± 3.500	0.856 ± 1.239	18.688 ± 3.801		0.002 ± 4.112
ACF	1.255 ± 2.771	0.259 ± 2.121	14.197 ± 3.618		2.792 ± 3.342
DOX : ACF (1 : 1)	4.162 ± 4.415	0.919 ± 1.279	32.063 ± 5.131	***	1.407 ± 2.349
DOX : ACF (1 : 2)	2.114 ± 4.982	0.467 ± 4.439	32.083 ± 4.021		2.714 ± 4.482
DOX : ACF (1 : 5)	1.765 ± 2.703	0.689 ± 3.408	18.296 ± 5.009	###	1.859 ± 3.087

cells (Fig. 6 right side) than to cancer cells (Fig. 6 left side). This is reflected in the IC50 values (Table 2).

Comparing the IC_{50} values for free compounds and their complexes for cancer cells, it was noted that the cytotoxicity of the complexes is comparable to the free drugs cytotoxicity. In contrast, DOX : ACF complexes (especially 1 : 1 and 1 : 2 ratios) have been observed to exhibit reduced cytotoxicity to non-cancerous cells compared to the free drugs. Reducing the toxicity to non-cancerous cells of an effective pre-cancer dose of doxorubicin is highly desirable due to its cardiotoxic properties, and taking into account the complementary mechanism of action of both compounds (incorporation into the DNA structure and inhibition of topoisomerase II), the use of acriflavine can increase the selective effect of DOX against cancer cells.

Since it was assumed that DOX : ACF complexes would be degraded in cancer cells, we decided to investigate the uptake of both free drugs and their complexes by cancer cells and non-cancer cells.

Uptake studies

To study the cellular uptake of doxorubicin, acriflavine and their complexes, cells were incubated with 1 μM compounds for 2, 24 and 48 hours. The observation of cellular uptake was possible due to fluorescent properties of analysed compounds. The fluorescence of doxorubicin and acriflavine could be observed independently, because both compounds emit different wavelengths, which was measured with a BD LSRII flow cytometer using a blue laser-488 nm with PE bandpass filter – 575/26 nm and FITC bandpass filter – 520/50 nm. Therefore, to make it easier to compare the rates of entry of the free drugs and the drugs in the complex, we decided to present them in one graph (Fig. 7). The curves show the entry rate of the free drugs, while the bars show the entry rate of the complexes (divided into both drugs/components). Thanks to the aforementioned ability to simultaneously measure the fluorescence of complexed doxorubicin and acriflavine, we were able to

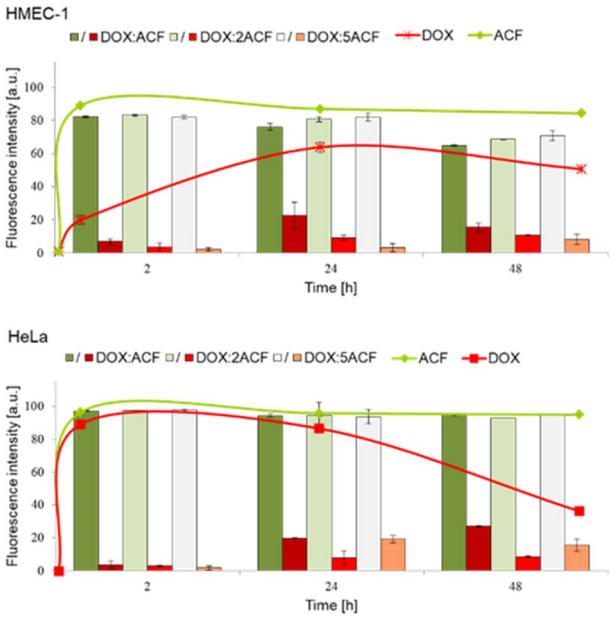

Fig. 7 The cellular uptake of the doxorubicin (DOX), acriflavine (ACF) and their complexes in molar ratios 1 : 1, 1 : 2 and 1 : 5 by human cervical cancer endothelial (HeLa) cells (lower panel) and dermal microvascular endothelium cells (HMEC-1) cells (upper panel) after 2, 24 and 48 h incubation in 310 K. Data are presented as a percentage of fluorescence ± standard deviation (SD). The statistical significance was assessed between free ACF and three complexes – green bars (*p < 0.05, **p < 0.01, ***p < 0.005, ****p < 0.001) as well as free DOX and three complexes – red bars ($^{\#}p$ < 0.05, $^{\#\#}p$ < 0.01, $^{\#\#\#}p$ < 0.005, $^{\#\#\#\#}p$ < 0.001).

assess whether the complex was stable or disintegrating. And if the complex was degrading, we could assess which drug was entering the cell faster.

As expected, both tested cell lines accumulated free compounds differently in contrast to the complexes, which entered the cells in a similar way. In the case of the non-cancerous cell line HMEC-1, the accumulation of free doxorubicin in the cells was much slower (maximum saturation was reached after 24 h of incubation) than in the case of free acriflavine, which reached the maximum saturation almost after administration (Fig. 5 upper panel – green and red line). In contrast, in the case of the HeLa cancer cell line, both free acriflavine and doxorubicin rapidly entered the cells and two hours after administration, both compounds showed maximum fluorescence (Fig. 5 lower panel – green and red line).

The next step was to study the entry rate of the three doxorubicin–acriflavine complexes into the cells. Two filters were used: PE (red) and FITC (green). In both cancer (HeLa) and non-cancer (HMEC-1) cells, the fluorescence intensity of the complexed acriflavine was comparable to free compound throughout the incubation period, from 2 to 48 hours (Fig. 7 – green bars and line).

At the same time, we observed that doxorubicin administered in a complex with acriflavine penetrates the cells much slower than the free compound. This may indicate that the complex decomposes at the stage of cell entry, and that both compounds compete with each other, because their mechanism of transport across the cell membrane is the same or equally efficient (as seen especially in the case of HeLa cells, where both free compounds enter equally quickly). In addition, after administration of the complexes, we observe the fluorescence intensity at the level of that of free acriflavine at full saturation (the fluorescence intensity is similar for each system, although the studied complexes differ in the amount of ACF). Paradoxically, this mechanism works in favour of the complexes, as they are less toxic to non-cancerous cells than to cancer cells, which is crucial for the combination of various drugs with cardiotoxic doxorubicin.

Experimental

Materials

Doxorubicin hydrochloride was obtained from Beijing Packbuy M&C, Beijing, China. Acriflavine (98%) was obtained from Apollo Scientific, UK. Dimethyl-d6-sulfoxide (99.8 at% D, ARMAR) and deuterium oxide (99.8 at% D, Sigma-Aldrich) were used as supplied by Merck.

Fluorescence analysis

Fluorescence was measured in quartz cuvettes using a HORIBA, Jobin Yvon spectrofluorometer. The samples were excited at 265 nm and their emission was observed from 450–700 nm. The widths of the excitation and emission slits were set to 3 nm. The samples were prepared by mixing constant concentration acriflavine (8 μM, Apollo Scientific, UK) and doxorubicin (Beijing Packbuy M&C, Beijing, China) at concentrations ranging from 0–30 μM in deionized water. Fluorescence measurements were made 24 hours after mixing acriflavine and doxorubicin.

NMR studies

Diffusion-Ordered Spectroscopy (DOSY) NMR spectra were recorded on Bruker Avance III 500 MHz instrument (Bruker BioSpin GmbH, Rheinstetten, Germany) equipped with 5 mm dual channel BBI probehead (^{1}H/^{2}H/BB) with z-gradients coil and GAB/2 gradient unit capable to produce B_0 gradients with maximum strength of 50 g cm^{-1}. The BCU-05 cooling unit, controlled by BVT3200 system, was used for temperature stabilization. DOSY experiments acquisition parameters were as follows: size of fid (TD): 16 384; spectral width (SW): 16.0214 ppm; acquisition time (AQ): 1.02 s; relaxation delay (D1): 3 s. DOSY experiments were run in pseudo 2D mode with 24 increments for gradient steps and 48 scans accumulated for each sub spectrum; gradients were changed between 5 and 95 percents of maximum strength. Spectra were accumulated and processed using Bruker TopSpin 3.2pl6 program running under Windows 7.

DOSY was used to measure and compare the diffusion coefficients of the ACF : DOX complex (ACF: 7.210^{-2} mg μl; DOX: 1.6 × 10^{-2} mg μl^{-1}) and free ACF (ACF: 7.2 × 10^{-3} mg μl^{-1}). Based on the knowledge of the diffusion coefficient (D) from DOSY and the Stokes–Einstein equation ($D = k_BT/6\pi\eta r$, k_B: Boltzmann constant, T: temperature, η: dynamic viscosity, r: hydrodynamic radius), the hydrodynamic radius of the ACF : DOX complex and free ACF were calculated and compared.

^{1}H NMR and ^{1}H–^{1}H ROESY spectra were recorded using Avance Neo 400 NMR spectrometer.

The Avance NEO 400 NMR spectrometer (Bruker Karlsruhe, Germany), operating at 400.15 MHz for ^{1}H, using 5 mm dual channel (^{1}H/^{2}H/BB) i-Probe (Bruker) operating with SampleCase Plus autosampler. The spectrometer uses a BCU-I, controlled by Bruker Smart Variable Temperature (BSVT) system, for the temperature regulation and stabilization. Spectra were accumulated using Bruker TopSpin 4.0.7 program running under Windows 10. ^{1}H NMR (298 K) analysis was performed in D_2O (0.9% saline). ACF, DOX and ACF : DOX solutions were prepared to final concentration 3.3×10^{-3} mg μl^{-1}, 7.5×10^{-3} mg μl^{-1} and 3.3×10^{-3}: 7.5×10^{-3} mg μl^{-1}, respectively. The ^{1}H NMR acquisition parameters were as follows: size of fid (TD): 65 536; spectral width (SW): 20.4840 ppm; acquisition time (AQ): 3.9 976 959 s; number of scans: 24 and relaxation delay (D1): 2 s. ^{1}H–^{1}H ROESY NMR acquisition parameters were as follows: data point matrix (TD2 × TD1): 4096–256 K; spectral width in both dimensions (SW1 and SW2): 15.6190 ppm; acquisition time (AQ): 0.3 276 800; number of scans per FID: 8; relaxation delay (D1 = 2 s). ACF, DOX and ACF : DOX solutions were prepared with the same concentrations as for the ^{1}H NMR spectra. For all spectra, the chemical shift was referenced using residual solvent peak, D_2O or DMSO, as reference (4.78 and 2.49 ppm, respectively).

The molar mass of acriflavine ($M = 468.98$ g mol^{-1}) equal to the sum of the molar masses of proflavine and trypaflavine was used for the calculations.

Determination of cytotoxicity

The influence of the doxorubicin (DOX), acriflavine (ACF) and complexes of these drugs in molar ratios 1 : 1, 1 : 2 and 1 : 5 on the cell viability was determined with the use of the MTT-assay.

Briefly, HMEC-1 and HeLa cells were seeded into 96-well plates at a density of 1.5×10^4 cells per well. After the cells adhere to the plate bottom (24 h), DOX, ACF and complexes at final concentrations of 1, 5, 10, 50 μM were added to medium. Cells were incubated with the compounds for 24 and 48 h in a 310 K humidified atmosphere containing 5% CO_2.

After the incubation period cells were washed with 100 μl of phosphate buffered saline (PBS). Next, 50 μl of a 0.5 mg mL^{-1} solution of MTT in PBS was added to each well and cells were further incubated under normal culture conditions for 3 h. After incubation the residue MTT solution was removed and the obtained formazan precipitate was dissolved in DMSO (100 μl per well). The conversion of the tetrazolium salt (MTT) to a colored formazan by mitochondrial and cytosolic dehydrogenases is a marker of cell viability. Before the absorbance measurement plates were shaken for 1 min and the absorbance at 570 nm was measured on the PowerWave HT Microplate Spectrophotometer (BioTek, USA).

Cellular internalization

The next step was evaluate the cellular uptake efficiency of DOX, ACF and complexes. For flow cytometry measurements, HeLa and HMEC-1 cells were seeded into a 12-well plate with 1×10^5 cells in each well and cultured overnight in proper medium (1 mL) containing 10% FBS at 37 °C with 5% CO_2.

Subsequently, the drugs and complexes (in final 1 μM concentration) were added into each well, followed by 2, 24 and 48 h incubation. After that, the medium was removed and the cells were washed with cold PBS (10 mM, 7.4). Then, the cells were detached by trypsin, collected by centrifugation, and suspended in proper medium (0.5 mL) for flow cytometry measurements. Analysis was performed with a Becton Dickinson LSRII flow cytometer (BD Biosciences, USA) using a blue laser-488 nm with PE bandpass filter – 575/26 nm and FITC bandpass filter – 520/50 nm.

Statistical analysis

For statistical significance testing, one-way ANOVA for concentration series and post hoc Tukey's test for pairwise difference testing were used. In all tests, p-values < 0.05 were considered to be statistically significant. Data are presented as arithmetic mean ± SD. The cytotoxicity values were related to the untreated control. The statistical significance was assessed between free DOX and three complexes (*p < 0.05, **p < 0.01, ***p < 0.005, ****p < 0.0001) as well as free ACF and three complexes at the same compound concentration or time of incubation ($^{\#}p$ < 0.05, $^{\#\#}p$ < 0.01, $^{\#\#\#}p$ < 0.005, $^{\#\#\#\#}p$ < 0.0001).

Conclusions

The interaction and cytotoxicity of the anti-cancer drugs acriflavine and doxorubicin were investigated as candidates for co-delivery of drugs in the treatment of cervical cancer. According to the data from fluorescence and NMR analyses, acriflavine and doxorubicin were observed to form complexes due to van der Waals forces, hydrogen bonding and π–π stacking. Computational studies confirm the thermodynamic ability of the system in question to form thermodynamically favorable ACF–DOX interactions and among them π–π interactions in particular. Moreover, it was shown that computations for acriflavine–doxorubicin complexation support the view that the latter complex is thermodynamically much more favorable than dimers of the acriflavine moieties, even if the basis set superposition error (BSSE) is taken into account. Biological studies showed statistically comparable activity of DOX : ACF systems and free compounds against the cancerous HeLa cell line and their reduced cytotoxicity against the non-cancer HMEC-1 cell line. At the same time, significantly more efficient cellular uptake of acriflavine than doxorubicin was noted, regardless of whether it was administered as a free compound or in combination with an anthracycline. The mechanism determining the selective toxicity of ACF : DOX complexes for non-cancerous and cancerous cells should be better understood in the future, as it may be of key importance when combining various drugs with cardiotoxic doxorubicin.

Author contributions

KP – developed the concept, carried out part of the synthetic work and interpreted NMR and fluorescence results and co-

wrote the manuscript; JK – carried out part of the synthetic work; BG – was responsible for computational studies; SK – was responsible for NMR analyses; WAS – provided useful suggestions for this project, supervised the studies and finally corrected the paper; MM, AJ – performed biological assays, compiled and described the results; BKM – supervised the biological studies and the correctness of the biological part of the paper.

Conflicts of interest

The authors declare no competing financial interest.

Acknowledgements

The acknowledgements come at the end of an article after the conclusions and before the notes and references. The authors thank the following funding institutions for financing the research: Centre of Molecular and Macromolecular Studies of Polish Academy of Sciences and Faculty of Biology and Environmental Protection, University of Lodz. Upgrade of the Avance III 500 NMR spectrometer used, to obtain results included in this publication, was supported by the founds from the EU Regional Operational Program of the Lodz Region, RPLD.01.01.00-10-0008/18. Purchase of the Avance Neo 400 NMR spectrometer, used to obtain results included in this publication, was supported by the founds from the EU Regional Operational Program of the Lodz Region, RPLD.01.01.00-10-0008/18.

Notes and references

1 B. Jawad, L. Poudel, P. Rudolf and C. Wai-Yim, *J. Phys. Chem. B*, 2020, **124**(36), 7803–7818, DOI: **10.1021/acs.jpcb.0c05840**.

2 K. Piorecka, K. Jan, M. Stanczyk and W. A. Stanczyk, Synthetic routes to nanomaterials containing anthracyclines: noncovalent systems, *Biomater. Sci.*, 2018, **6**(10), 2552–2565, DOI: **10.1039/C8BM00739J**.

3 K. Piorecka, D. Smith, K. Jan, M. Stanczyk, A. Wlodzimierz and W. A. Stanczyk, Synthetic routes to nanoconjugates of anthracyclines, *Bioorg. Chem.*, 2020, **96**, 103617, DOI: **10.1016/j.bioorg.2020.103617**.

4 D. Agudelo, P. Bourassa, G. Bérubé and H.-A. Tajmir-Riahi, Intercalation of antitumor drug doxorubicin and its analogue by DNA duplex: Structural features and biological implications, *Int. J. Biol. Macromol.*, 2014, **66**, 144–150, DOI: **10.1016/j.ijbiomac.2014.02.028**.

5 B. Jawad, L. Poudel, P. Rudolf, N. F. Steinmetze and C. Wai-Yim, Molecular mechanism and binding free energy of doxorubicin intercalation in DNA, *Phys. Chem. Chem. Phys.*, 2019, **21**, 3877–3893, DOI: **10.1039/C8CP06776G**.

6 P. Singh Rawat, A. Jaiswal, K. Amit, J. Singh Bhatti and U. Navik, Doxorubicin-induced cardiotoxicity: An update on the molecular mechanism and novel therapeutic strategies for effective management, *Biomed. Pharmacother.*, 2021, **139**, 111708, DOI: **10.1016/j.biopha.2021.111708**.

7 C. Christowitz, T. Davis, A. Isaacs, G. Van Niekerk, S. Hattingh and A.-M. Engelbrecht, Mechanisms of doxorubicin-induced drug resistance and drug resistant tumour growth in a murine breast tumour model, *BMC Cancer*, 2019, **19**, 757, DOI: **10.1186/s12885-019-5939-z**.

8 J. E. S. Shay, H. Z. Imtiyaz, S. Sivanand, A. C. Durham, S. Nicolas, S. Hsu, M. Vera, T. S. K. Eisinger-Mathason, B. L. Krock, D. N. Giannoukos and M. C. Simon, Inhibition of hypoxia-inducible factors limits tumor progression in a mouse model of colorectal cancer, *Carcinogenesis*, 2014, **35**(5), 1067–1077, DOI: **10.1093/carcin/bgu004**.

9 S. Ramakrishnan, V. Anand and S. Roy, Vascular Endothelial Growth Factor Signaling in Hypoxia and Inflammation, *J. Neuroimmune Pharmacol.*, 2014, **9**, 142–160, DOI: **10.1007/s11481-014-9531-7**.

10 B. L. Krock, S. Nicolas and M. C. Simon, Hypoxia-induced angiogenesis: good and evil, *Genes Cancer*, 2011, **2**(12), 1117–1133, DOI: **10.1177/1947601911423654**.

11 G. Dong, X.-H. Lin, H.-H. Liu, D.-M. Gao, J.-F. Cui, Z.-G. Ren and R.-X. Chen, Intermittent hypoxia alleviates increased VEGF and pro-angiogenic potential in liver cancer cells, *Oncol. Lett.*, 2019, **18**(2), 1831–1839, DOI: **10.3892/ol.2019.10486**.

12 K. Chatterjee, J. Zhang, H. Norman and J. S. Karliner, Doxorubicin Cardiomyopathy, *Cardiology*, 2010, **115**, 155–162, DOI: **10.1159/000265166**.

13 L. Xu, Z. Zhang, Y. Ding, L. Wang, Y. Cheng, L. Meng, J. Wu, A. Yuan, Y. Hu and Y. Zhu, Bifunctional liposomes reduce the chemotherapy resistance of doxorubicin induced by reactive oxygen species, *Biomater. Sci.*, 2019, **7**, 4782, DOI: **10.1039/c9bm00590k**.

14 K. A. Lee, H. Zhang, D. Z. Qian and G. L. Semenza, Acriflavine inhibits HIF-1 dimerization, tumor growth, and vascularization, *Proc. Natl. Acad. Sci. U.S.A.*, 2009, **106**(42), 17910–17915, DOI: **10.1073/pnas.0909353106**.

15 P. J. Jodłowski, K. Dymek, G. Kurowski, J. Jaśkowska, W. Bury, M. Pander, S. Wnorowska, K. Targowska-Duda, W. Piskorz, A. Wnorowski and A. Boguszewska-Czubara, Zirconium-Based Metal–Organic Frameworks as Acriflavine Cargos in the Battle against Coronaviruses – A Theoretical and Experimental Approach, *ACS Appl. Mater. Interfaces*, 2022, **14**(25), 28615–28627, DOI: **10.1021/acsami.2c06420**.

16 V. Napolitano, A. Dabrowska, K. Schorpp, A. Mourão, E. Barreto-Duran, M. Benedyk, P. Botwina, S. Brandner, M. Bostock, Y. Chykunova, C. Anna, G. Dubin, T. Fröhlich, M. Hölscher, M. Jedrysik, A. Matsuda, K. Owczarek, M. Pachota, P. Oliver, P. Jan and K. Pyrc, Acriflavine, a clinically approved drug, inhibits SARS-CoV-2 and other betacoronaviruses, *Cell Chem. Biol.*, 2022, **29**, 774–784, DOI: **10.1016/j.chembiol.2021.11.006**.

17 R. Nehme, R. Hallal, M. El Dor, F. Kobeissy, F. Gouilleux, F. Mazurier and K. Zibara, Repurposing of Acriflavine to Target Chronic Myeloid Leukemia Treatment, *Curr. Med. Chem.*, 2020, **28**(11), 2218–2233, DOI: **10.2174/0929867327666200908114411**.

18 D. Sabolova, P. Kristian and M. Kozurkova, Proflavine/acriflavine derivatives with versatile biological activities, *J. Appl. Toxicol.*, 2020, **40**, 64–71, DOI: 10.1002/jat.3818.

19 R. K. Tubbs, W. E. Ditmars Jr. and Q. Van Winkle, Heterogeneity of the interaction of DNA with acriflavine, *J. Mol. Biol.*, 1964, **9**(2), 545–557, DOI: 10.1016/S0022-2836(64)80226-6.

20 G. Pépin, C. Nejad, B. J. Thomas, J. Ferrand, K. McArthur, P. G. Bardin, R. Bryan, G. Williams and M. P. Gantier, Activation of cGAS-dependent antiviral responses by DNA intercalating agents, *Nucleic Acids Res.*, 2017, **45**(1), 198–205, DOI: 10.1093/nar/gkw878.

21 M. Wainwright, Acridine—a neglected antibacterial chromophore, *J. Antimicrob. Chemother.*, 2001, **47**(1), 1–13, DOI: 10.1093/jac/47.1.1.

22 S. Seredinski, F. Boos, S. Günther, J. A. Oo, T. Warwick, J. I. Ponce, F. F. Lillich, E. Proschak, S. Knapp, R. Gilsbach, B. Pflüger-Müller, R. P. Brandes and M. S. Leisegang, DNA topoisomerase inhibition with the HIF inhibitor acriflavine promotes transcription of lncRNAs in endothelial cells, *Mol. Ther.–Nucleic Acids*, 2022, **27**, 1023–1035, DOI: 10.1016/j.omtn.2022.01.016.

23 M. K. Gatasheh, S. Kannan, K. Hemalatha and N. Imrana, Proflavine an acridine DNA intercalating agent and strong antimicrobial possessing potential properties of carcinogen, *Karbala Int. J. Mod. Sci.*, 2017, **3**(4), 272–278, DOI: 10.1016/j.kijoms.2017.07.003.

24 D. Roth, M. London and M. Manjon, Binding Specificity and Affinity of Acriflavine for Nucleic Acids, *Stain Technol.*, 1967, **42**(3), 125–132, DOI: 10.3109/10520296709114994.

25 L. M. Chan and Q. Van Winkle, Interaction of acriflavine with DNA and RNA, *J. Mol. Biol.*, 1969, **40**(3), 491–495, DOI: 10.1016/0022-2836(69)90167-3.

26 K. Piorecka, K. Jan and A. Wlodzimierz, Stanczyk, Acriflavine, an Acridine Derivative for Biomedical Application: Current State of the Art, *J. Med. Chem.*, 2022, **65**(17), 11415–11432, DOI: 10.1021/acs.jmedchem.2c00573.

27 C. C.-L. Wong, H. Zhang, D. M. Gilkes, J. Chen, W. Hong, P. Chaturvedi, M. E. Hubbi and G. L. Semenza, Inhibitors of hypoxia-inducible factor 1 block breast cancer metastatic niche formation and lung metastasis, *J. Mol. Med.*, 2012, **90**, 803–815, DOI: 10.1007/s00109-011-0855-y.

28 L. Meng, Y. Cheng, X. Tong, S. Gan, Y. Ding, Y. Zhang, C. Wang, L. Xu, Y. Zhu, J. Wu, Y. Hu and A. Yuan, Tumor Oxygenation and Hypoxia Inducible Factor-1 Functional Inhibition via a Reactive Oxygen Species Responsive Nanoplatform for Enhancing Radiation Therapy and Abscopal Effects, *ACS Nano*, 2018, **12**(8), 8308–8322, DOI: 10.1021/acsnano.8b03590.

29 A. Bulle, J. Dekervel, L. Libbrecht, D. Nittner, L. Deschuttere, D. Lambrecht, E. Van Cutsem, C. Verslype and J. Van Pelt, Gemcitabine induces Epithelial-to-Mesenchymal Transition in patient-derived pancreatic ductal adenocarcinoma xenografts, *Am. J. Transl. Res.*, 2019, **11**(2), 765–779.

30 J. Zhou, Y. Li, L. Wang and Z. Xie, Mimetic sea cucumber-shaped nanoscale metal-organic frameworks composite for enhanced photodynamic therapy, *Dyes Pigm.*, 2022, **197**, 109920, DOI: 10.1016/j.dyepig.2021.109920.

31 A. Mangraviti, T. Raghavan, F. Volpin, S. Nicolas, D. Gullotti, J. Zhou, L. Asnaghi, E. Sankey, A. Liu, Y. Wang, D.-H. Lee, N. Gorelick, R. Serra, M. Peters, D. Schriefer, F. Delaspre, F. J. Rodriguez, C. G. Eberhart, B. Henry, A. Olivi and B. Tyler, HIF-1α- Targeting Acriflavine Provides Long Term Survival and Radiological Tumor Response in Brain Cancer Therapy, *Sci. Rep.*, 2017, **7**, 14978, DOI: 10.1038/s41598-017-14990-w.

32 R. Martí-Díaz, M. F. Montenegro, J. Cabezas-Herrera, C. R. Goding, J. N. Rodríguez-López and L. Sánchez-del-Campo, Acriflavine, a Potent Inhibitor of HIF-1α, Disturbs Glucose Metabolism and Suppresses ATF4-Protective Pathways in Melanoma under Non-Hypoxic Conditions, *Cancers*, 2021, **13**, 102, DOI: 10.3390/cancers13010102.

33 J. Liu, J. Zhang, X. Wang, Y. Li, Y. Chen, K. Li, J. Zhang, L. Yao and G. Guo, HIF-1 and NDRG2 contribute to hypoxia-induced radioresistance of cervical cancer Hela cells, *Exp. Cell Res.*, 2010, **316**(12), 1985–1993, DOI: 10.1016/j.yexcr.2010.02.028.

34 P. Zargar, E. Ghani, F. J. Mashayekhi, R. Amin and E. Eftekhar, Acriflavine enhances the antitumor activity of the chemotherapeutic drug 5-fluorouracil in colorectal cancer cells, *Oncol. Lett.*, 2018, **15**(6), 10084–10090, DOI: 10.3892/ol.2018.8569.

35 F. Ibrahim, H. Elmansi and R. Aboshabana, Assessment of two analgesic drugs through fluorescence quenching of acriflavine as a new green methodology, *Microchem. J.*, 2021, **164**, 105882, DOI: 10.1016/j.microc.2020.105882.

36 D. Dagher, H. Elmansi, J. J. Nasr and N. El-Enany, Utility of a novel turn-off fluorescence probe for the determination of tranilast, an adjunctive drug for patients with severe COVID-19, *RSC Adv.*, 2022, **12**, 22044–22053, DOI: 10.1039/D2RA02239G.

37 M. Tolba and H. Elmansi, Studying the quenching resulted from the formation of an association complex between olsalazine or sulfasalazine with acriflavine, *R. Soc. Open Sci.*, 2021, **8**, 210110, DOI: 10.1098/rsos.210110.

38 C. Manivannan, S. Sambathkumar and R. Renganathan, Interaction of acriflavine with pyrimidines: A spectroscopic approach, *Spectrochim. Acta, Part A*, 2013, **114**, 316–322, DOI: 10.1016/j.saa.2013.05.034.

39 L. I. A. Ali, A. F. Qader, M. I. Salih and H. Y. Aboul-Enein, Sensitive spectrofluorometric method for the determination of ascorbic acid in pharmaceutical nutritional supplements using acriflavine as a fluorescence reagent, *Luminescence*, 2019, **34**, 168–174, DOI: 10.1002/bio.3589.

40 C. Manivannan, K. Meenakshi Sundaram, M. Sundararaman and R. Renganathan, Investigation on the inclusion and toxicity of acriflavine with cyclodextrins: a spectroscopic approach, *Spectrochim. Acta, Part A*, 2014, **122**, 164–170, DOI: 10.1016/j.saa.2013.11.012.

41 C. Manivannan, S. Baskaran, P. Vijayakumar and R. Renganathan, Spectroscopic investigation and computational studies on the interaction of Acriflavine

with various estrogens, *Spectrochim. Acta, Part A*, 2019, **206**, 622–629, DOI: 10.1016/j.saa.2018.07.047.

42 L. Xu, Z. Zhang, Y. Ding, Li Wang, Y. Cheng, L. Meng, J. Wu, A. Yuan, Y. Hu and Y. Zhu, Bifunctional liposomes reduce the chemotherapy resistance of doxorubicin induced by reactive oxygen species, *Biomater. Sci.*, 2019, **7**, 4782–4789, DOI: 10.1039/C9BM00590K.

43 R. Wang, Y. Yang, M. Yang, D. Yuan, J. Huang, R. Chen, H. Wang, L. Hu, L. Di and J. Li, Synergistic inhibition of metastatic breast cancer by dual-chemotherapy with excipient-free rhein/DOX nanodispersions, *J. Nanobiotechnol.*, 2020, **18**, 116, DOI: 10.1186/s12951-020-00679-2.

44 K. Piorecka, K. Jan, I. Bak-Sypien, M. Cypryk, U. Steinke and W. A. Stanczyk, Reasons for enhanced activity of doxorubicin on co-delivery with octa(3-aminopropyl)silsesquioxane, *RSC Adv.*, 2020, **10**, 15579–15585, DOI: 10.1039/d0ra01319f.

45 K. Piorecka, J. Anna, M. Majkowska, M. Marcinkowska, K. Jan, S. Kazmierski, E. Radzikowska-Cieciura, B. Kost, P. Sowinski, B. Klajnert-Maculewicz and W. A. Stanczyk, Hydrophilic Polyhedral Oligomeric Silsesquioxane, $POSS(OH)_{32}$, as a Complexing Nanocarrier for Doxorubicin and Daunorubicin, *Materials*, 2020, **13**(23), 5512, DOI: 10.3390/ma13235512.

46 K. Piorecka, K. Jan and W. A. Stanczyk, Novel Polyhedral Silsesquioxanes $[POSS(OH)_{32}]$ as Anthracycline Nanocarriers—Potential Anticancer Prodrugs, *Molecules*, 2021, **26**(1), 47, DOI: 10.3390/molecules26010047.

47 K. Piorecka, W. Stanczyk and M. Florczak, NMR analysis of antitumor drugs: Doxorubicin, daunorubicin and their functionalized derivatives, *Tetrahedron Lett.*, 2017, **58**(2), 152–155, DOI: 10.1016/j.tetlet.2016.11.118.

48 P. Groves, Diffusion ordered spectroscopy (DOSY) as applied to polymers, *Polym. Chem.*, 2017, **8**, 6700–6708, DOI: 10.1039/C7PY01577A.

49 A. D. Becke, Density-functional thermochemistry. III. The role of exact exchange, *J. Chem. Phys.*, 1993, **98**(7), 5648, DOI: 10.1063/1.464913.

50 S. Grimmea, J. Antony, S. Ehrlich and H. Krieg, A consistent and accurate ab initio parametrization of density functional dispersion correction (DFT-D) for the 94 elements H-Pu, *J. Chem. Phys.*, 2010, **132**(15), 154104, DOI: 10.1063/1.3382344.

51 M. J. Frisch, G. W. Trucks, H. B. Schlegel, G. E. Scuseria, M. A. Robb, J. R. Cheeseman, G. Scalmani, V. Barone, G. A. Petersson, H. Nakatsuji, X. Li, M. Caricato, A. V. Marenich, J. Bloino, B. G. Janesko, R. Gomperts, B. Mennucci, H. P. Hratchian, J. V. Ortiz, A. F. Izmaylov, J. L. Sonnenberg, D. Williams-Young, F. Ding, F. Lipparini, F. Egidi, J. Goings, B. Peng, A. Petrone, T. Henderson, D. Ranasinghe, V. G. Zakrzewski, J. Gao, N. Rega, G. Zheng, W. Liang, M. Hada, M. Ehara, K. Toyota, R. Fukuda, J. Hasegawa, M. Ishida, T. Nakajima, Y. Honda, O. Kitao, H. Nakai, T. Vreven, K. Throssell, J. A. Montgomery Jr., J. E. Peralta, F. Ogliaro, M. J. Bearpark, J. J. Heyd, E. N. Brothers, K. N. Kudin, V. N. Staroverov, T. A. Keith, R. Kobayashi, J. Normand, K. Raghavachari, A. P. Rendell, J. C. Burant, S. S. Iyengar, J. Tomasi, M. Cossi, J. M. Millam, M. Klene, C. Adamo, R. Cammi, J. W. Ochterski, R. L. Martin, K. Morokuma, O. Farkas, J. B. Foresman, and D. J. Fox, *Gaussian 16 Rev. C.01*, Wallingford, CT, 2016.

52 S. F. Boys and F. Bernardi, The calculation of small molecular interactions by the differences of separate total energies. Some procedures with reduced errors, *Mol. Phys.*, 1970, **19**(4), 553–566, DOI: 10.1080/00268977000101561.